International Journal of Hydrogen Energy 58 (2024) 56–68

Contents lists available at ScienceDirect

International Journal of Hydrogen Energy

journal homepage: www.elsevier.com/locate/he

Techno-economic analysis and optimization of hydrogen production from renewable hybrid energy systems: Shagaya renewable power plant-Kuwait

Wisam K. Hussam [a,b,*], El Manaa Barhoumi [c], M. Abdul-Niby [d], Gregory J. Sheard [b]

[a] Mechanical Engineering Department, Australian University, Safat, Kuwait
[b] Department of Mechanical and Aerospace Engineering, Monash University, VIC 3800, Australia
[c] Department of Electrical and Computer Engineering, Dhofar University, Salalah, Oman
[d] Electrical and Electronics Engineering Department, Australian University, Safat, Kuwait

ARTICLE INFO

Keywords:
Hybrid energy system
Photovoltaic
Wind turbine
Hydrogen
Fuel cells
Optimization

ABSTRACT

The present study examines the potential for hydrogen production using the hybrid energy system at the Shagaya renewable power plant. Techno-economic and optimization analyses are used to identify the optimum configurations that reduce costs while increasing the renewable fraction and lowering greenhouse gas emissions. Three configurations were considered, exploring on- and off-grid combinations of photovoltaic solar (PV), wind turbine (WT), fuel cells and batteries. Integrating PV solar with wind power connected to the power grid was found to achieve the lowest levelized cost of energy of 0.539 \$/kWh and a hydrogen production cost of 6.85 \$/kg. However, for the stand-alone system where battery storage banks or fuel cells are used, the cost of hydrogen increases to more than 8.0 \$/kg due to the larger capital cost of the system. The optimized system achieves annual green hydrogen production of 111 877 kg along with an annual carbon dioxide emission reduction of 14 819 kg. A sensitivity analysis proves that COE is more sensitive to PV price than wind turbines and electrolyzers. LCOE falls by 32.3% to 0.365 kWh when the PV unit price drops to 50%. The LCOE falls by 4% to 0.517 kWh when WT costs decrease by 50%.

1. Introduction

Awareness of the environmental impact of humanity's reliance on fossil fuels has progressively increased over recent years, motivating efforts towards sustainable development and reducing carbon emissions. Hydrogen is a clean and efficient alternative to fossil fuels, with potential applications in power generation, transportation, and industrial processes. However, its production is energy intensive. Renewable energy sources offer a solution to this dilemma. Studies estimate that hydrogen energy will meet 11% of global energy demand by 2025 and 34% by 2050, and project that renewable production of hydrogen has significant potential to meet global hydrogen demand [1]. To achieve this, cost-effective and sustainable methods for renewable hydrogen production, such as via wind or solar power, need to be developed.

Production costs render hydrogen relatively expensive compared to other energy sources. A disadvantage of either solar or wind power for hydrogen production is the intermittency of the generated power. Nasser et al. [2] suggests that a hybrid approach that integrates both wind and solar power may serve as a viable solution to reduce costs. Utilizing a hybrid system increases the efficiency of hydrogen-production due both to the elevated electricity input to and higher water temperature within the electrolyzer [3]. Electrolyzers utilize electricity to split water into hydrogen and oxygen. Furthermore, incorporating a battery system into the system setup reduces the number of electrolyzer cutoffs while simultaneously increasing working hours, efficiency, and overall lifespan [4]. The hybrid system's utilization factor exceeds that of a standalone system [5]. Further information may be found in the reviews by Qazi et al. [6] and Al-Enezi et al. [7].

Various forms of sustainable energy resources can be utilized independently or in conjunction with alternative energy sources to provide a reliable system that meets the required energy demands [8]. Photovoltaic-wind hybrid energy systems, which combine solar photovoltaic (PV) and wind turbines (WT), have been shown to have a high energy output and lower instability than standalone solar or wind systems. Furthermore, integrating such hybrid systems can decrease the expenses incurred in electricity generation and mitigate intermittency problems related to renewable energy sources [9]. The Shagaya renewable power plant located in Kuwait's western region, where sunlight and wind are abundant, is an example of a hybrid energy system that utilizes a range of sustainable resources such as solar, wind, and

* Corresponding author at: Mechanical Engineering Department, Australian University, Safat, Kuwait.
E-mail address: w.alsaadi@au.edu.kw (W.K. Hussam).

https://doi.org/10.1016/j.ijhydene.2024.01.153
Received 11 October 2023; Received in revised form 27 December 2023; Accepted 14 January 2024

Acronyms and nomenclature

COE	Cost of Energy
COH	Cost of Hydrogen
CRF	Capital Recovery Factor
FC	Fuel Cell
GHG	Greenhouse Gas
GWe	Gigawatt-electric
HOMER	Hybrid Optimization of Multiple Energy Resources
HTank	Hydrogen Tank
kWh	Kilowatt-hour
LCOE	Levelized Cost of Energy
LCOH	Levelized Cost of Hydrogen
MWh	Megawatt-hour
NPC	NetPresent Cost
NREL	National Renewable Energy Laboratory
O&M	Operation and Maintenance
PEM	Proton Exchange Membrane
PV	Photovoltaic
RF	Renewable Fraction
WT	Wind Turbine

thermal power to generate electricity, with plans to achieve 3.2 GWe by 2030 [10].

Availability of solar and wind resources is key to the efficacy of renewable energy systems. The location of Shagaya offers an advantage in terms of solar resources, with a mean daily yield of 5.2 kWh/m^2 and around 9.2 h of maximum annual sun exposure per day [11]. It has an average capacity factor of 21.5%, which is slightly higher than the reported range for wind technology of 10–21% [12]. The wind resource at Shagaya is also promising, with estimated speeds of 5–7 m/s [13]. The average capacity factor for wind power at Shagaya is 45% [13], which is slightly higher than the reported range of 23–44% [14] for wind technology. With these favourable conditions, renewable energy production could be achieved at a lower cost than in other countries, reducing production costs for green hydrogen. Several studies have sought the optimal configuration of hybrid PV-WT-H_2 systems [15–21]. Comprehensive reviews of PV-WT hybrid systems pertaining to hydrogen production are given in Alzahrani et al. [17] and Nasser et al. [22]. These demonstrate that integrating solar and wind power with water electrolysis yields substantial enhancements in hydrogen production efficiency.

The feasibility of a hybrid system comprised of 10 kW wind turbines and a 1 kWp solar array connected to electrolyzers for hydrogen production was analysed by Akyuz et al. [15]. TRNSYS, MATLAB, and HOMER were used to optimize the system. The investigation revealed that the hybrid system achieved 60% efficiency in hydrogen production, surpassing the efficiency levels of standalone wind or PV systems.

An extensive techno-economic analysis conducted by Hasan and Genç [16] examined the viability of a hybrid system based in Iraq employing solar and wind power. This system comprises wind turbines with power ratings ranging from 500 kW to 2 GW. It is complemented by two types of solar panels, namely 330 W and 315 W. Furthermore, integrating electrolyzers with different power ratings is an essential component of the solar/photovoltaic (PV) hybrid system. These electrolyzers comprise 18 units rated at 48 kW, four at 215 kW, two at 430 kW, and one at 860 kW. The study determined that the system achieved a maximum annual hydrogen production quantity of 49 150 m^3H_2. The corresponding cost for hydrogen production under these conditions was calculated to be 0.752 $\$/m^3H_2$. However, by selling the surplus energy the system generates back to the grid, the production cost can be reduced to 0.723 $\$/m^3H_2$.

Important metrics used to evaluate hybrid systems include the cost of energy (COE), the cost of hydrogen (COH), the levelized cost of hydrogen (LCOH), and the net present cost (NPC).

Okonkwo et al. [19] investigated the possibility of generating green hydrogen using a hybrid energy system in Salalah, Oman, integrating wind, solar, hydrogen storage tanks, and fuel cells. Economic viability was demonstrated, with conditions minimizing both LCOH and COE being determined.

A techno-economic evaluation was conducted into hybrid systems in Al-Kharj, Saudi Arabia, by Okonkwo et al. [21], utilizing HOMER software to compare and evaluate sets of renewable energy sources for optimal electricity generation and hydrogen production. A photovoltaic array, inverter, wind turbine, electrolyzer, and hydrogen tank were all part of the investigated hybrid system. The optimized hybrid energy system minimized LCOH, LCOE and NPC.

Although there have been several studies on solar and wind potential in Kuwait, [7,23–27], studies assessing their deployment in hybrid hydrogen production systems are scarce. Therefore, this study aims to conduct a techno economic analysis of hydrogen production via a solar-wind hybrid energy system at the Shagaya power plant. The levelized cost method will be used to ascertain the costs of producing energy and hydrogen. The analysis will assess system feasibility from both a technical and economic perspective, and will provide insights into the potential of renewable hydrogen production using hybrid energy systems. The Shagaya Renewable Power Plant is situated in a location abundant in solar energy and wind. However, no comprehensive assessment of the primary renewable energy sources in this region of Kuwait has been conducted thus far. This study's findings will guide policymakers and industry stakeholders in promoting the green hydrogen production in Kuwait and beyond.

The paper is structured as follows: Section 2 provides information on the system location and meteorological data. In Section 3, the methodology is outlined, encompassing system components, optimization and economic criteria, levelized cost of energy, and sensitivity analysis. The findings and subsequent discussion are detailed in Section 4, while Section 5 concludes the paper.

2. Geographical location and meteorological data

The Shagaya power plant is located at 29.2055°N and 47.0524°E in Kuwait, approximately 100 km west of Kuwait City, as depicted in Fig. 1. Meteorological data for the Shagaya site was obtained from the NASA Surface Metrology and Solar Energy database and utilized as inputs for the hybrid power system modelling software employed in this study. Fig. 2. presents the monthly mean wind speed, temperature, and solar radiation profiles for the Shagaya site.

Fig. 2(a) depicts the monthly mean solar radiation, where high-intensity solar radiation can be seen between May and August. The yearly mean solar irradiance is 5.40 $kWh/m^2/day$. In December, the minimum recorded daily solar irradiance reaches approximately 2.65 $kWh/m^2/day$, while the highest occurs in June, surpassing 7.89 $kWh/m^2/day$. Fig. 2(b) illustrates the monthly average temperature fluctuation, depicting a range between 12.57 °C and 37.6 °C. The fluctuation in wind velocity is elucidated in Fig. 2(c). The peak wind speed of 5.75 m/s occurs in June, while the lowest wind speed of 4.22 m/s, occurs in October. Bedoud et al. [28] explain that a threshold wind speed, the cut-in speed, must be surpassed to generate substantial electricity. Cut-in speeds of 3 m/s are common for wind turbines commonly found in wind parks [21]. The wind speeds observed in this study range from 4.22 m/s to 5.75 m/s, which are therefore adequate for the generation of electricity.

The solar radiation and wind speed distributions clearly demonstrate high photovoltaic and wind turbine potentials at the site under study.

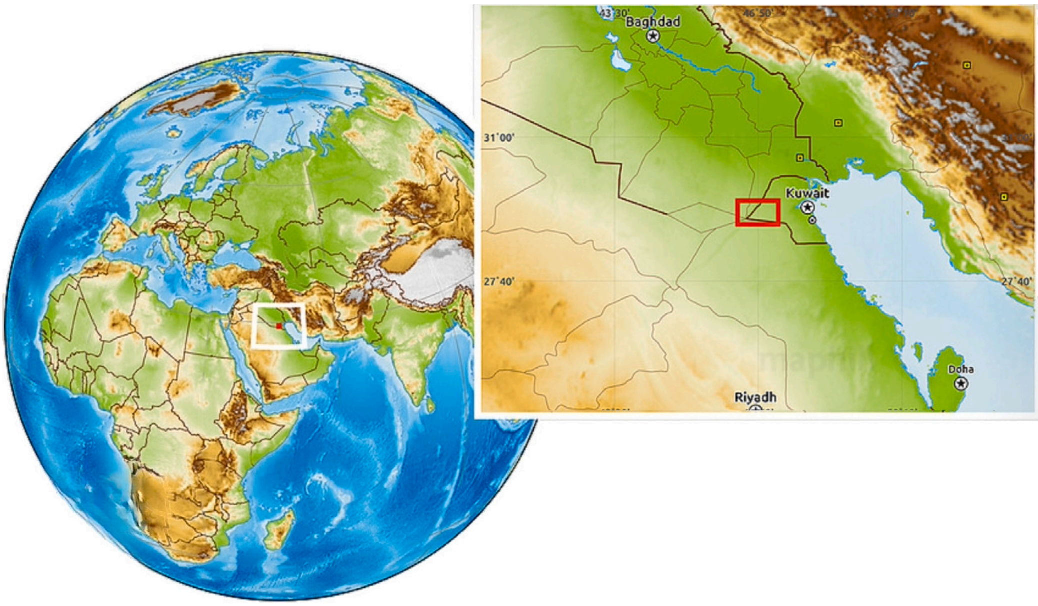

Fig. 1. The geographical location of Shagaya power plant in Kuwait.

3. Methodology

The current hybrid energy system aims to produce 300 kg/day of green hydrogen by harnessing solar and wind power to produce electrical energy and hydrogen, which are subsequently stored and utilized for generating electricity to supply the load demand. Fig. 3 illustrates a simplified diagram of the proposed hybrid system.

3.1. System components

The renewable energy system considered in the present study comprises electricity generation via PV and WT, an inverter, an electrolyzer (EL), storage via a battery and a hydrogen tank (HTank), and a fuel cell (FC). The configuration of elements of a hybrid energy system has been shown to considerably impact the efficiency and amount of power produced [29].

3.1.1. Photovoltaic module

PV modules arrange individual PV cells in series to achieve a specified output voltage, and in parallel to generate sufficient electric current. Output power is determined by incident solar radiation and panel temperature, and may be expressed as

$$P_{PV} = Y_{PV} f_{PV} \frac{G_T}{G_S} \left[1 + \beta (T_c - T_{ref})\right], \tag{1}$$

where G_T is the incident solar irradiation under standard test conditions, Y_{PV} is the module's rated capacity, f_{PV} is the derating factor, $T_{ref} = 25$ °C is the cell temperature under standard test conditions and $0.004 \lesssim \beta \lesssim 0.005/$ °C is the temperature coefficient [30].

Mono-crystalline PV panels were employed for the Shagaya PV plant, and the cost is obtained from Solar Choice [31]. Technical and economical parameters for the PV panel under consideration are provided in Table 1.

3.1.2. Wind turbine

The electrical power generated by wind turbines is calculated using the manufacturer-provided characteristic curve, which correlates with the wind speed at the turbine's hub height

$$\frac{u}{u_0} = \left(\frac{z}{z_0}\right)^{\alpha}, \tag{2}$$

where the wind speed at z above the ground is represented by u. The wind speed measured at the reference height $z_o = 10$ m is denoted by u_o, while α is a coefficient of friction that relates to the ground surface. The power produced by the wind turbine can be mathematically described by a curve fitting to its characteristic curve [20] as

$$P_w(u) = \begin{cases} 0 & \text{for} \rightarrow \quad u < u_c \\ a_1 u^n \ldots b_1 u^2 + c_1 u + d_1 & \text{for} \rightarrow \quad u_c \le u < u_1 \\ a_2 u^n \ldots b_2 u^2 + c_2 u + d_2 & \text{for} \rightarrow \quad u_1 \le u < u_2 \\ a_3 u^n \ldots b_3 u^2 + c_3 u + d_3 & \text{for} \rightarrow \quad u_2 \le u < u_f \\ a_3 u^n \ldots b_3 u^2 + c_3 u + d_3 & \text{for} \rightarrow \quad u > u_f \end{cases} \tag{3}$$

where $P_w(u)$ is the wind turbine output power at wind speed u. u_c and u_f are the respective turbine cut-in and cut-out speeds, u_1 and u_2 are intermediate wind speed levels used to increase curve fitting accuracy. The parameters of the chosen wind turbine are listed in Table 1.

3.1.3. Electrolyzer

The most viable process to generate hydrogen using renewable resources is water electrolysis. It has been demonstrated that the highest efficiency can be obtained when water electrolysis is employed in conjunction with a photovoltaic array in a hybrid configuration [32]. A proton exchange membrane (PEM) was used in this study, and Table 1 lists the technical parameters of the model electrolyzer used herein.

3.1.4. Hydrogen tank

Energy storage systems can be utilized to overcome the energy supply shortage during the night and seasonal discrepancies caused by solar energy. In the present system, a storage tank is used to store surplus hydrogen when production exceeds demand. Studies have demonstrated that the potential for hydrogen storage to serve as an economically and environmentally sustainable alternative for energy storage surpasses that of conventional battery storage over extended periods [33]. The details of the storage tank can be found in Table 1. The details outlining the storage tank's specifications are listed in Table 1.

3.1.5. Fuel cell

A Proton Exchange Membrane (PEM) fuel cell is employed to convert chemical energy into electrical energy through an electrochemical process. Utilizing an external fuel source (hydrogen in this case), the energy released through oxidation is transformed into electricity, heat,

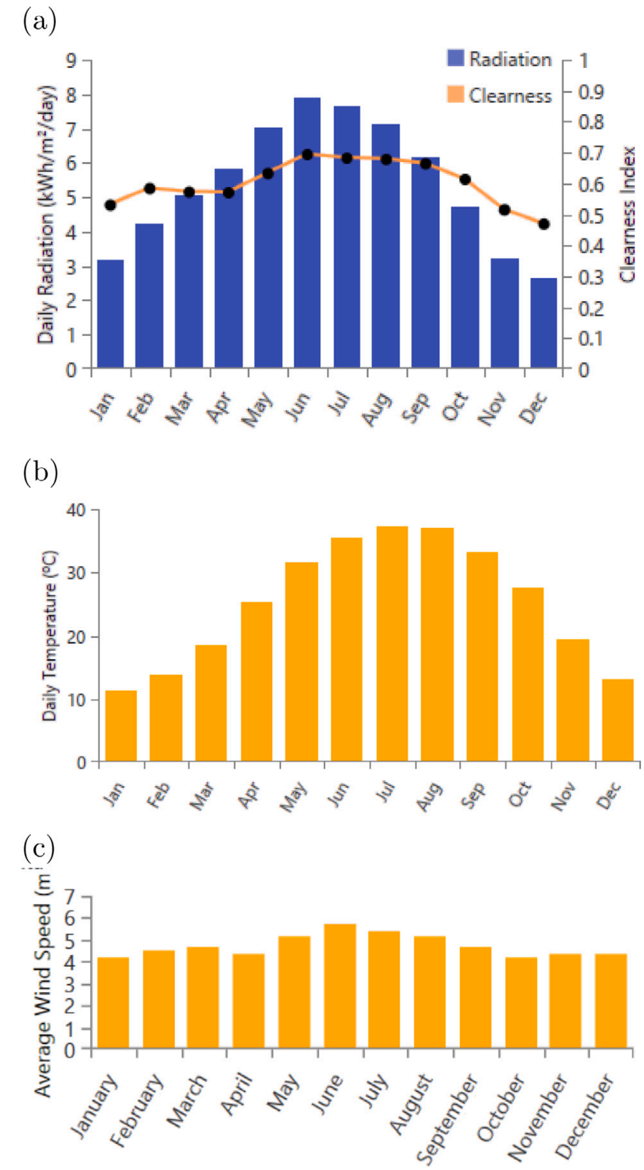

Fig. 2. Plots showing the monthly mean climatic conditions at the plant location, showing (a) solar radiation and clearness, (b) ambient temperature and (c) wind speed.

and water without emitting pollutants. The integration of fuel cells with sustainable energy sources like PV and WT enhances system sustainability by shifting electricity generation to periods of low renewable energy availability. The viability of incorporating fuel cells with PV systems has been successfully demonstrated in both on-grid and off-grid applications [34]. The technical and economical characteristics are given in Table 1.

3.1.6. Battery bank

The surplus energy produced by the hybrid system is stored in a battery bank for times when the demand for electricity surpasses the supply from the PV, WT, and FC components. The capacity of the battery bank during its charging phase, occurring when the power generated by the hybrid system exceeds its required load, is represented over time by a specific function [20] by

$$C_B(t) = C_B(t-1)(1-\sigma) + \left(P_T(t) - \frac{P_L(t)}{\eta_{conv}} \right) \eta_{Batt}, \tag{4}$$

Table 1
Specifications for the system elements.

Photovoltaic		Wind turbine	
Parameter	*Value*	*Parameter*	*Value*
Model	Generic	Model	XANT 330
Efficiency	20%	Cut-in speed	3 m/s
Capacity	1 kW	Cut-out speed	24 m/s
Capital cost	$1000/kW	Capacity	330 kW
Replacement cost	$1000/kW	Capital cost	$50 000/kW
O&M cost	$10/year	Replacement cost	$50 000/kW
Lifetime	25 years	O&M cost	$500/year
		Lifetime	20 years
Electrolyzer		**Hydrogen tank**	
Parameter	*Value*	*Parameter*	*Value*
Model	PEM	Capital cost	$100/kg
Efficiency	85%	Replacement cost	$100/kg
Capacity	1 kW	O&M cost	$1/year
Capital cost	$500/kW	Lifetime	25 years
Replacement cost	$400/kW		
O&M cost	$20/year		
Lifetime	15 years		
Fuel cell		**Battery, Inverter**	
Parameter	*Value*	*Parameter*	*Value*
Model	PEM	Model	Li-Ion, ABB MGS100
Efficiency	50%	Efficiency	90%, 95%
Capacity	1 kW	Capacity	1 kWh, 1 kW
Capital cost	$3000/kW	Capital cost	$550/kW, $500/kW
Replacement cost	$2500/kW	Replacement cost	$550/kW, $500/kW
O&M cost	$10/year	O&M cost	$0.01/h, $1/year
Lifetime	50000 h	Lifetime	15 years

while capacity during discharge (where the load demand exceeds the power generated) is given by

$$C_B(t) = C_B(t-1)(1-\sigma) + \left(\frac{P_L(t)}{\eta_{conv}} - P_T(t) \right). \tag{5}$$

Here P_T represents the overall power output generated by the system, P_L denotes the load demand at the specific hour, σ signifies the self-discharge rate of the battery bank, η_{Batt} reflects the discharging efficiency of the battery bank, and η_{conv} stands for the converter efficiency. The specifications for the battery are outlined in Table 1.

3.1.7. Inverter

An inverter transforms a direct-current electrical supply (here from PV and WT) into an alternating current output to the electrical grid. The inverter also manages the charging and discharging of the batteries, ensuring that excess energy is stored and used when needed. The technical specifications of the inverter are given in Table 1.

3.2. Simulations and optimization criteria

This study employs the HOMER Pro software package [35] to simulate, model, optimize, and conduct sensitivity analysis on the power system under investigation. It is a software specifically created for the modelling and optimization of microgrid systems, making it an excellent tool for assessing and improving the performance of renewable energy systems. Its adaptability stems from its capacity to consider diverse renewable energy sources, storage technologies, and system topologies allow a thorough study. It takes a techno-economic optimization method that considers both technical and economic characteristics to provide a comprehensive prospective of the design and operation of renewable energy systems. The software for hybrid renewable energy generation systems was developed by the National Renewable Energy Laboratory (NREL) in the United States. It has been validated and employed in many hybrid energy systems, for example, Ma et al. [36], Abdin and Mérida [37], Okonkwo et al. [19,21]. This package streamlines the evaluation of designs for off-grid and on-grid energy

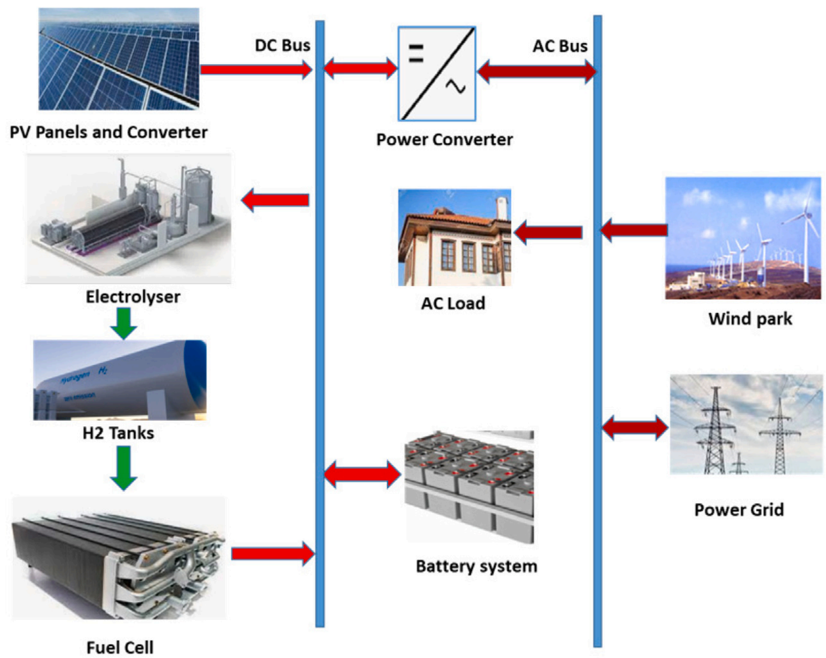

Fig. 3. Schematic diagram of a hybrid solar system for hydrogen production.

systems across multiple applications. HOMER Pro operates by seeking an equilibrium between energy generation and consumption at each time step throughout the year. The simulation process involves the identification of technically feasible system configurations within the predefined constraints.

Additionally, it estimates the installation and operational costs associated with the feasible system over the project's lifespan. The optimization process in HOMER Pro requires essential input data, such as load profiles, solar resources specific to the chosen location, and technical and economic details of the system components. The optimized configuration of the system is designed to meet the load demand, focusing on net present cost (NPC), cost of energy (COE), and system reliability. Fig. 4 illustrates a flowchart detailing the optimization steps within HOMER.

At the start, the electricity and hydrogen loads, along with the renewable energy resources of the site, are defined. The software utilizes the data specified in Table 1 to determine the optimal dimensions for the electrolyzers, hydrogen storage tanks, PV systems, WT, battery banks, and power converters.

3.2.1. *Hybrid energy system configurations*

Three different system configurations are considered during the simulations, as shown in Fig. 5: on-grid-PV-WT, off-grid-PV-WT with battery and off-grid-PV-WT with fuel cell. In the first configuration, the PV panels and wind turbines are integrated with electrolyzers, power converters, hydrogen tanks and a power grid. As depicted in Fig. 5(a), this system connects the PV-WT system to the power grid, providing electricity to loads during periods of low solar availability and wind speed. An advantage of the grid-connected PV system is the capability to sell surplus electricity generated back to the power grid. Fig. 5(b) illustrates the standalone PV-WT system integrated with batteries for electricity storage. This configuration operates independently of the conventional power grid; therefore, battery units are required to supply electricity to the load during insufficient wind and solar energy. The power generated by the PV panels and wind turbines meets the load demand, with the electrolyzer taking the excess electricity to produce hydrogen that is then stored in the hydrogen tank. The third configuration involves using fuel cells to produce electricity from hydrogen, as depicted in Fig. 5(c). If the hybrid system power generated by the hybrid system generates insufficient electricity during periods of reduced solar irradiance and low winds, the fuel cells are employed to meet demand.

3.2.2. *Load profile*

The hydrogen demand in the system is anticipated to be fulfilled by producing hydrogen through electrolysis. Photovoltaic panels or wind turbines generate the required electrical energy to power the electrolyzer for hydrogen production. HOMER evaluates the necessary load by analysing meteorological data specific to the location. It provides two approaches for estimating the load profile daily or with step-by-step randomness [21]. The daily profiles of electrical and hydrogen loads used in this analysis are depicted in Fig. 6. The highest daily loads for electricity and hydrogen occur between 04:00—16:00 and 06:00—17:00, respectively.

3.3. *Economic analysis criteria*

The feasibility of the hybrid system is evaluated using the net present cost (NPC), levelized cost of energy (LCOE), and levelized cost of hydrogen (LCOH). HOMER computes the NPC, LCOE and LCOH, arranging them in descending order of cost based on the optimized results.

3.3.1. *Net present cost of the hybrid system*

NPC is obtained from analysis of the total expenses associated with a project, including capital, operating and maintenance cost. The NPC over the project lifetime is calculated as [38,39]

$$\mathrm{NPC} = \frac{C_{\mathrm{ann,\ tot}}}{\mathrm{CRF}(i,n)}, \tag{6}$$

$$C_{\mathrm{ann,\ tot}} = C_{\mathrm{cap}} + C_{\mathrm{rep}} + C_{\mathrm{O\&M}} - R_{\mathrm{salv}}, \tag{7}$$

$$i = \frac{\acute{i} - f}{1 - f}, \tag{8}$$

$$\mathrm{CRF} = \frac{i(1+i)^n}{(1+i)^n - 1}, \tag{9}$$

where $C_{\mathrm{ann,\ tot}}$ (\$/year) represents the total annual cost, CRF is the capital recovery factor, i is the annual interest rate (%), and n is the lifetime of the hybrid system. $C_{\mathrm{ann,\ tot}}$, C_{rep}, $C_{\mathrm{O\&M}}$ and R_{salv} represent the total

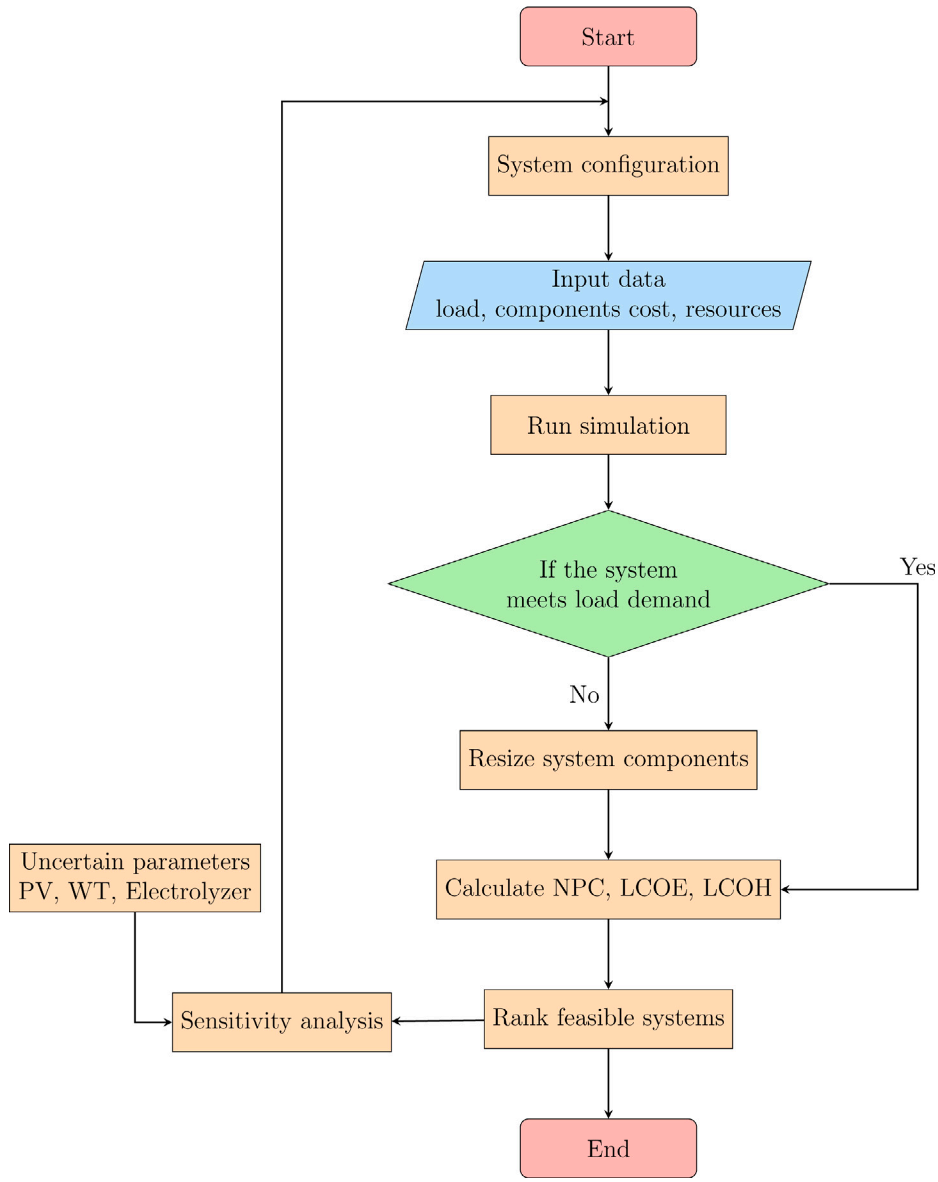

Fig. 4. Flowchart depicting the optimization process within HOMER Pro.

annual cost, replacement cost, total operating and maintenance cost and salvage value, while the nominal interest rate is í and the annual inflation rate is f.

3.3.2. Levelized cost of energy

The LCOE of the hybrid system is a key metric that assesses the economic feasibility of a system. It is computed by adding all costs associated with the power plant over its lifetime, including initial investment, operation and maintenance, fuel, and other relevant expenditures, then translating these costs to an equivalent per-unit cost of electricity. The LCOE is the ratio of the total annual cost ($) to the total energy generated by the system (kWh) and is defined [40] as

$$\text{LCOE} = \frac{C_{\text{ann,tot}}}{E_{\text{tot}}}. \tag{10}$$

3.3.3. Levelized cost of hydrogen

The LCOH is used to assess the viability of an energy system. It represents the average cost of producing and delivering a unit of hydrogen over the system's lifetime, considering capital costs, operating and maintenance expenses, and the system lifespan. It is calculated by dividing the total annual cost ($) by the annual hydrogen production (kg H_2) as [41]

$$\text{LCOH} = \frac{C_{\text{ann,tot}}}{M_{H_2}}, \tag{11}$$

where LCOH and M_{H_2} represent the levelized cost of hydrogen ($/kg H_2) and annual hydrogen produced (kg/year).

3.4. Sensitivity analysis

In optimizing the hybrid energy system size, parameters such as wind velocity, solar irradiance, the cost of purchasing electricity from the grid, and the expenses associated with system components may exhibit fluctuations and uncertainties. These uncertainties can have an impact on the optimization outcomes, as well as the final LCOH. A sensitivity analysis is conducted to test the response of the system to changes in the input cost. This study considers the variability of component costs of the wind turbine and PV array. The electrolyzer's lifetime effect on the levelized energy and hydrogen supply costs is also analysed. Wind turbine and PV cost multipliers of (0.6–1) and (7–20) lifetime of electrolyzer are considered.

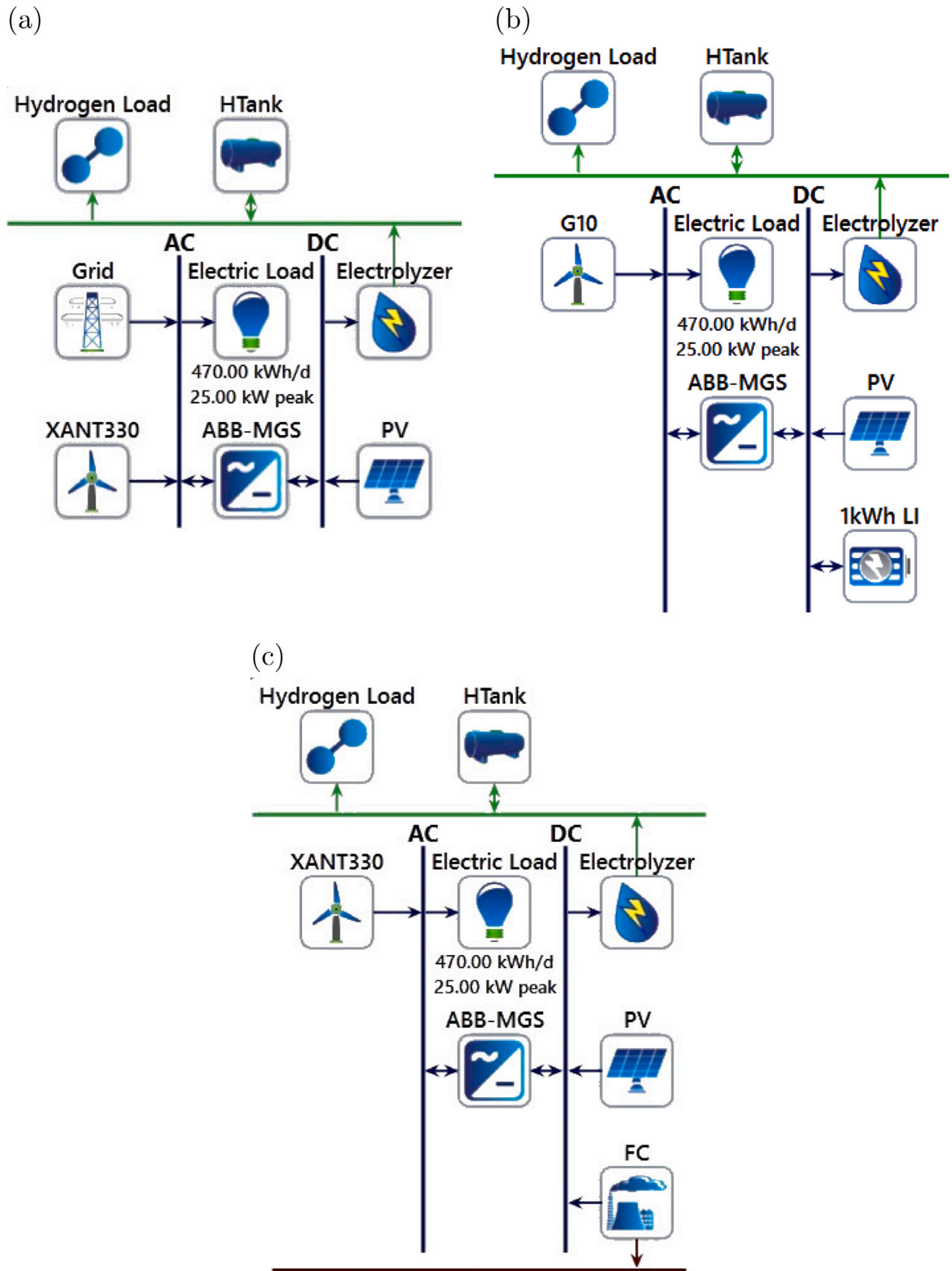

Fig. 5. Schematic layouts of the tested hybrid energy systems: (a) grid-connected PV-WT, (b) standalone PV-WT with battery, and (c) PV-WT with fuel cell.

4. Results and discussion

Results are presented in four subsections. First, the size of each optimized system is determined with respect to the optimization parameters such as NPC, COE and COH. This is followed by consideration of cost analysis and electricity and hydrogen production. Finally, the sensitivity analyses are presented.

4.1. System optimization

In the current study, three different system configurations, namely off-grid-PV-WT-battery, on-grid-PV-WT and off-grid-PV-WT-FC were examined. HOMER models all potential combinations for the hybrid energy system to identify the most efficient solution that fulfils the load requirements with minimal Levelized Cost of Energy (COE) and Net Present Cost (NPC), while maximizing the Renewable Fraction (RF) and minimizing greenhouse gas (GHG) emissions. The configurations presented in Fig. 5 are considered in the optimization process. The software requires inputs such as capital cost, O&M cost, replacement cost, lifetime, and efficiency of system components. The parameter values are presented in Table 1.

In addition to the mentioned optimization techniques, there are several others, such as the Mayfly Algorithm, genetic algorithm (GA), CUKO Search, Grey Wolf, Constrained Particle Swarm Optimization (CPSO), Harmony Search (HS), and Flower Pollination Algorithm (FPA) [42–44]. These techniques offer diverse approaches to optimization, but their effectiveness can vary depending on the system's complexity and the specific problem being addressed. When selecting an optimization technique, it is essential to consider factors such as convergence speed, sensitivity to initial conditions, and applicability. Ultimately, the chosen technique should align with the characteristics of the renewable

Table 2
Technical and economical comparison of different system configurations.

System	I: *on-grid*	II: *off-grid*	III: *off-grid*
Components	PV, WT, Inverters, Electrolyzers, HTank	PV, WT, Inverters, HTank, Electrolyzers, Batteries	PV, WT Inverters, Electrolyzers, HTank, FC
PV capacity	6395 kW	6432 kW	8287 kW
WT capacity	660 kW	990 kW	990 kW
Renewable energy fraction	98.4%	100%	100%
Yearly produced hydrogen	111 877 kg	111 905 kg	116 903 kg
Total NPC	9.91M $	11.61M $	13.68M$
Operating cost	77 659.30 $	174 342.30 $	189 798.70 $
Initial capital	8.91M $	9.36M $	11.20M $
LCOE	0.539 $/kWh	5.23 $/kWh	6.18 $/kWh
LCOH	6.85 $/kg	8.02 $/kg	9.06 $/kg

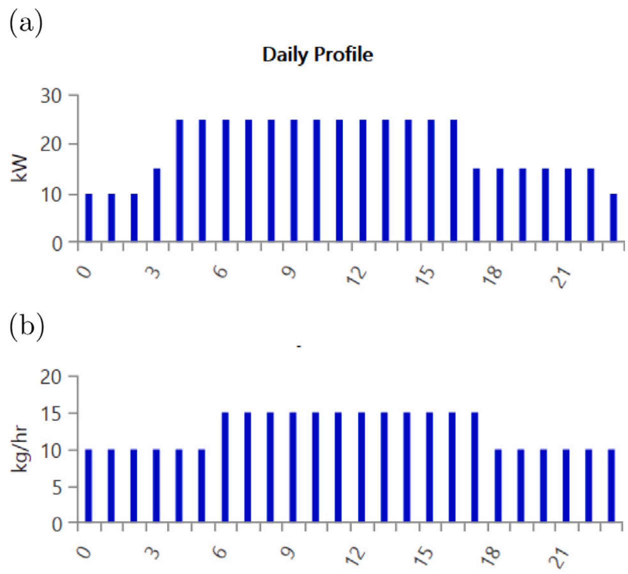

Fig. 6. Daily load profiles of (a) electricity and (b) hydrogen plotted over a representative 24-hour day.

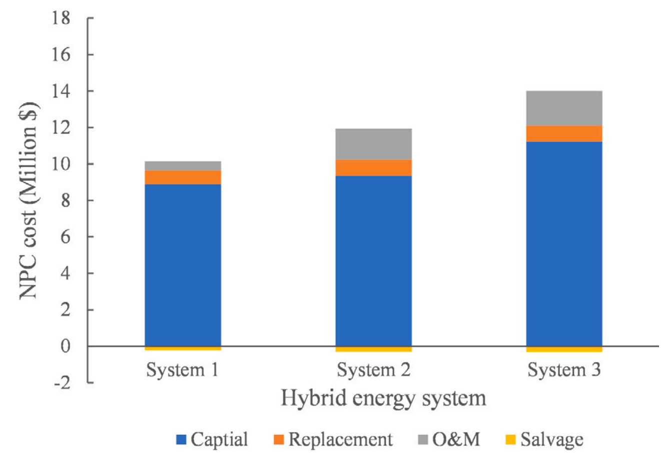

Fig. 7. Cost summary for systems 1–3 grouped by cost type.

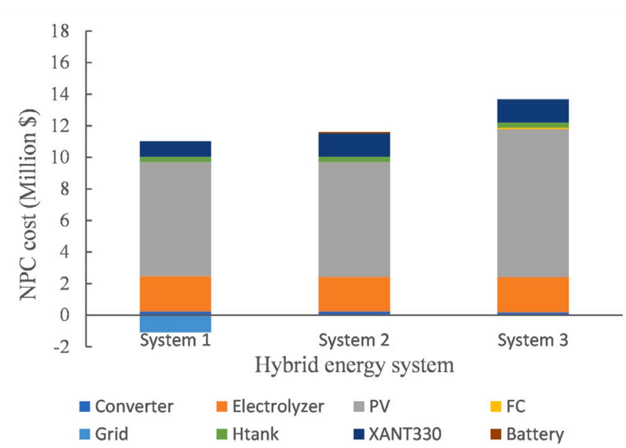

Fig. 8. Cost summary for systems 1–3 grouped by component type.

energy system, including its complexity, non-linearity, and limitations. While these alternative methodologies provide valuable contributions, the optimization tool selection should be guided by the unique features of the renewable energy system being studied.

The components, sizes, and economic parameters of the optimum system configurations determined by dodeling are given in Table 2. The results presented in Table 2 demonstrate that the grid-connected system is the optimal choice when considering the cost of the system, cost of energy and cost of hydrogen. It exhibits the lowest NPC, COE and COH and therefore is considered the best-optimized system. It comprises 6395 kW of photovoltaic power, two wind turbine units, a 2500 kW electrolyzer, a 3000 kg hydrogen tank and a 337 kW inverter.

The NPC for this system is $9.91M with a capital cost of $8.91M, whereas the NPC of the standalone off-grid-PV-WT with batteries and with fuel cells are respectively $11.61M and $13.68M. The standalone PV-WT integrated with batteries exhibits a lower net present cost than the standalone PV-WT combined with fuel cells. Nonetheless, the NPC of the standalone PV-WT with batteries remains higher than the NPC of the grid-connected PV-WT. The LCOE and LCOH for the optimized hybrid configuration were 0.539 $/kWh and 6.85 $/kg, respectively.

4.2. Cost analysis

Fig. 7 illustrates the optimized hybrid system NPC results. Capital costs exceed 82% of the overall NPC, with replacement and O&M costs trailing behind. The O&M cost associated with a component accounts for the expenses related to its operation and maintenance. Additionally, the grid O&M cost represents the annual expenditure for purchasing electricity from the grid, with any revenue generated from selling power back to the grid subtracted. Given that the amount of electricity sold back to the grid significantly surpasses the electricity obtained from the grid, the O&M cost in the on-grid system is notably reduced by over $130 000 compared to the off-grid system.

The cash flow of all the components analysed in the hybrid systems is depicted in Fig. 8. It can be noted that the PV and electrolyzer have the highest costs, almost 70% and 20% of the total cost. The grid components positively impact the total NPC cost of system 1. Compared to systems 2 and 3, the total NPC of system 1 is lower by almost 1.7 M *and* 3.78M, respectively. This is mainly because the capital cost of system 1 is 5% lower than system 2 and 26% lower than system 3.

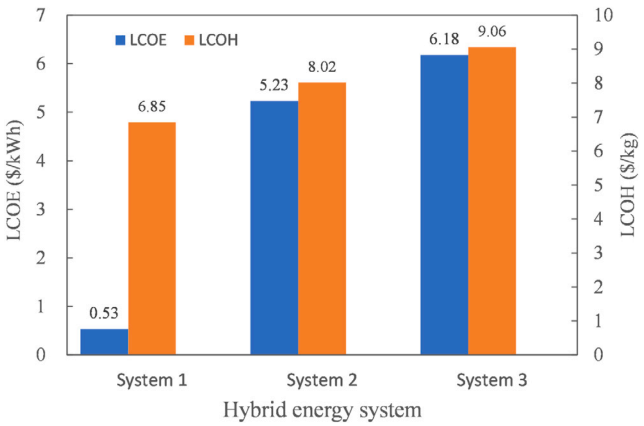

Fig. 9. Electrolyzer lifetime effect on LCOH.

Fig. 9 shows the overall LCOE and LCOH for the considered hybrid systems. The LCOE and LCOH for system 1 were, respectively, 0.539 $/kWh and 6.85 $/kg, whereas system 3 exhibits the highest LCOE and LCOH of 6.18 $/kWh and 9.06 $/kg, followed by system 2 with LOCE of 5.23 $/kWh and LCOH of 8.02 $/kg. The LCOE of the standalone hybrid systems is substantially greater than local feed-in tariffs, demonstrating that PV-WT grid-connected systems would be viable for electrical and hydrogen production.

4.3. Electricity and hydrogen production

The monthly average electricity generation from the photovoltaic modules, wind turbine and the power grid for the system with the optimal configuration is presented in Fig. 10(a). It can be noted that the electricity produced by the PV and WT systems far exceeds the amount purchased from the power grid. In fact, the renewable energy penetration fraction, which represents the proportion of renewable energy used compared to total energy consumption, is remarkably high at 98%, demonstrating a substantial contribution of renewable energy to the system. Approximately 1.25 MWh per year of surplus PV and WT electricity is sold back to the grid, contributing to the overall renewable energy supply. In contrast, only 23 433 kWh annually is purchased from the grid during low solar and wind energy production periods. Furthermore, the result demonstrates that the PV system accounted for 92.4% (10.75 MWh) of the total electricity generated, while the wind turbine contributed 860 146 kWh (7.39%) to the annual electricity production. This finding is consistent with Fig. 13(a), which illustrates that the PV system was the primary electricity producer, significantly contributing to the overall power generation.

Figure Fig. 10(b) illustrates that the PV system generates more power during the midday hours and summer months of the year owing to the higher solar irradiance and extended duration of equivalent sun hours. Conversely, PV is incapable of generating any power during nighttime, represented by the black shading in the figure. The PV system starts generating electricity at around 8:00 a.m., with daily production of 29 455 kWh and peak power of 6 366 kW produced between 12:00 and 1:00 p.m. Wind turbines, in contrast, can produce power throughout the entire year, although their peak performance is similarly observed during the summer months as shown in Fig. 10(c). The capacity factor (CF) quantifies how effectively energy sources are utilized, and is defined as the ratio of the actual energy generated over a period of time by the installed capacity. Here the CF of the PV and WT elements are respectively 19.2% and 15%. These compare well to those reported in the literature [19,21].

The optimized system is configured with a 2 500 kW electrolyzer, yielding an annual hydrogen output of 111 877 kg while consuming 46.4 kWh of energy per kilogram of hydrogen. The electrolyzer exhibits a mean and a maximum output of 12.8 kg/h and 53.9 kg/h, respectively. Despite the electrolyzer's rated and maximum capacities standing at 2 500 kW, its mean power input measures 593 kW. The electrolyzer operated for a total of 7 030 h within a year and consumed 5 100 MWh of energy generated by renewable sources, and this energy consumption results in a capacity factor of 23.7%. From these inputs, the average power output of the electrolyzer across the year is calculated as 175 kW, which agrees well with the seasonal mean depicted in Fig. 11(a). The proposed system generates hydrogen on-site by utilizing the wind and solar renewable resources, thereby mitigating many of the challenges associated with transporting and distributing the hydrogen. The hydrogen reservoir integrated within the system starts the year with 300 kg of hydrogen (10% of total capacity). It concludes the year with 2 786 kg (92.8%), indicating that the system can sustain continuous operation from one year to the next. Fig. 11(b) presents the annual variation in the hydrogen tank's liquid level, clearly indicating that with the start of daylight, the tank's liquid level experiences a discernible rise, reaching near maximum capacity by the onset of evening.

4.4. Sensitivity analysis

The expense of hydrogen production is primarily influenced by the levelized cost of energy (LCOE), which is highly dependent on the PV and wind turbine expenses. Therefore, analysing the impact of variations in PV and wind turbine costs on LCOE is imperative. A cost multiplier parameter can be utilized to represent a range of costs relative to a baseline case for PV and wind turbines. Examining cost multipliers across a range of values provides insights into how fluctuations in PV and wind turbine costs affect overall LCOE and, in turn, the cost of hydrogen production through electrolysis. Fig. 12 illustrates the impact to the energy cost of changes of the PV and WT costs. As depicted in Fig. 12, the LCOE exhibits a linear relationship with both PV and wind turbine costs. The results also show that COE costs are significantly more sensitive to PV cost than wind turbines. For example, for system 1, when the PV unit price dropped to 50%, LCOE dropped by 32.3% and became 0.365 $/kWh, while it only dropped by 4% and became 0.517 $/kWh for a 50% decrease in WT cost. Similarly, system 2 fell by 27.7% and 3.9% and became 3.785 $/kWh and 5.190 $/kWh, respectively. For system 3, it dropped by 30.3% and 4% and became 4.308 $/kWh and 4.967 $/kWh, respectively. Systems 1 to 3 were therefore respectively 8.1, 7.1 and 7.5 times more sensitive to PV versus wind turbine cost.

The electrolyzer is a critical component of hybrid energy systems and a major capital investment. However, the lifetime of most proton exchange membrane (PEM) electrolyzers is currently only about 7 years, significantly shorter than the lifetime of the electrolyzers used in the present study, which is 15 years. This difference in lifetime will significantly impact the cost of hydrogen production as well as the cost of hydrogen supply. Fig. 13 displays the effect of electrolyzer lifetime on LCOH for three different systems. The data clearly shows that longer electrolyzer lifetimes correlate with lower LCOH for all three systems. This demonstrates the significance of electrolyzer lifetime in reducing overall hydrogen production costs. Extending electrolyzer life from 7 to 20 years reduces LCOH substantially by over 10% for System 1 and nearly 8% for Systems 2 and 3. The LCOH reductions start steeply as lifetime increases from 7 to 9 years, but the curve gradually flattens out at the higher lifetimes. Furthermore, it was found that when the lifetime of the electrolyzer was less than 12 years, system 1 demonstrated a clear economic benefit compared to the other two systems. This implies that generating hydrogen via a grid-connected photovoltaic-wind hybrid energy system may be viable in regions with abundant renewable resources.

The Levelized Cost of Hydrogen (LCOH) for a grid-connected system is influenced by the expenses associated with purchasing and selling

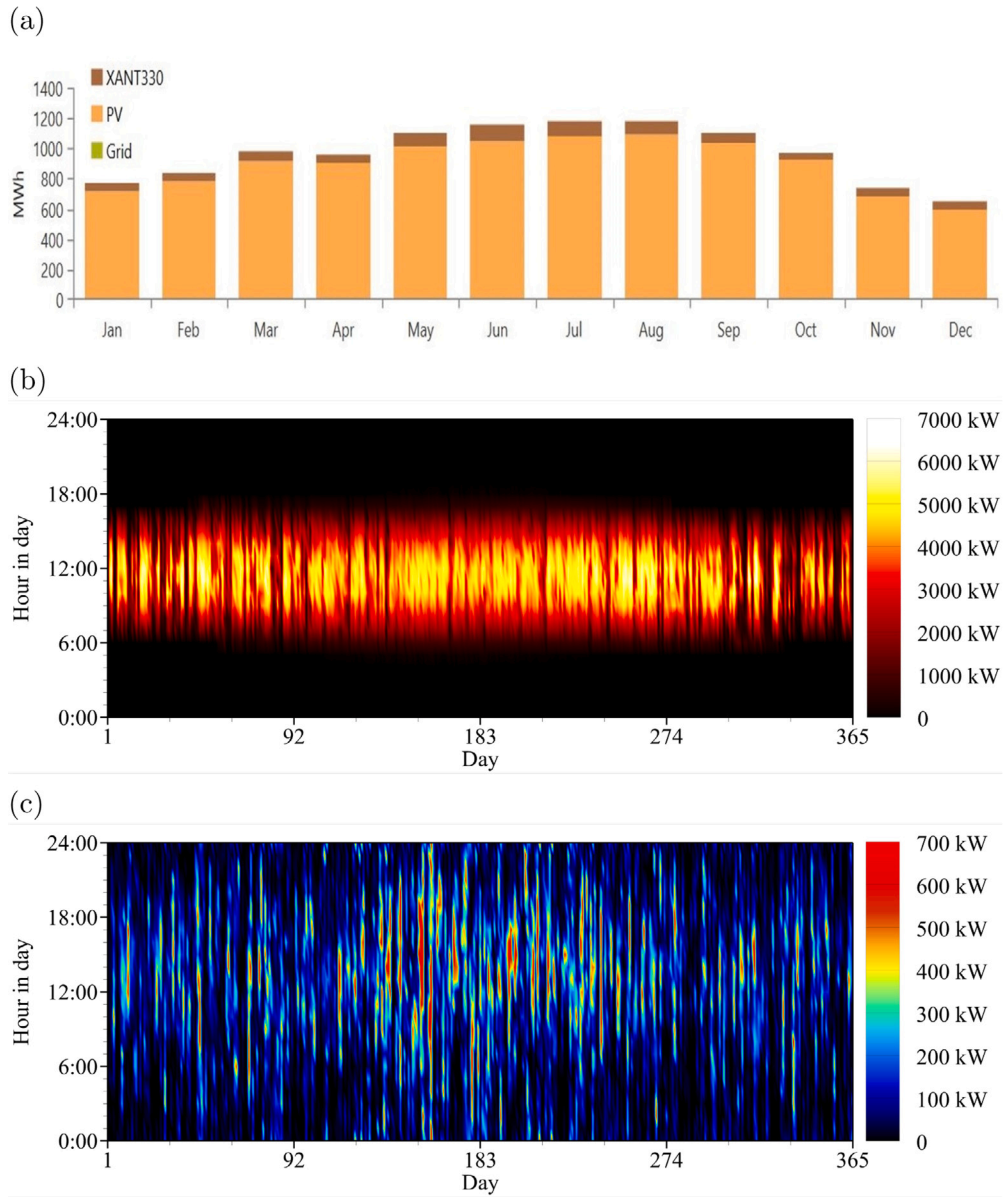

Fig. 10. (a) Monthly average electricity production. Annual (365/24) energy output (b) PV and (c) wind turbine in the optimum system.

energy to the grid. The results of capacity optimization indicate that the electricity acquired from the grid constitutes a minimal fraction, merely 0.2%, of the overall electricity consumption. However, the electricity sold back to the grid contributes significantly, accounting for 11% of the total power consumption. Consequently, the examination primarily focuses on assessing the impact of power prices when selling electricity back to the grid, as it plays a crucial role in determining the cost of hydrogen production throughout the system's operational lifespan. If the prices for electricity sold back to the grid increase, the levelized cost of hydrogen will decrease proportionally. The outcomes of the sensitivity analysis demonstrated that there is a linear correlation between LCOH and PV, wind turbine and electricity prices. It was found that LCOH dropped by almost 6% when the tariff-in feed increased by 50%.

5. Conclusion

In this study, the Shagaya renewable power plant was analysed for the techno-economic feasibility of producing hydrogen from renewable hybrid energy systems. The analysis considered three system configurations: off-grid using photovoltaic (PV), wind turbine (WT), and battery; on-grid using PV and WT; and off-grid using PV, WT, and fuel cell (FC). The main objective of the analysis was to determine the optimal solution that would minimize the Cost of Energy (COE), cost of hydrogen (COH), and Net Present Cost (NPC), while maximizing the Renewable Fraction (RF) and minimizing greenhouse gas (GHG) emissions.

The results showed that the grid-connected system, encompassing 6 395 kW of PV power, two wind turbines, a 2 500 kW electrolyzer, a 3 000 kg hydrogen tank, and a 337 kW inverter, emerged as the most favourable option due to its lowest NPC, COE, and cost of hydrogen (COH). Capital costs emerged as the most substantial component of the overall NPC, followed by replacement and operation and maintenance (O&M) costs. The O&M expenses of the grid-connected system were reduced by selling back its surplus electricity to the grid. Furthermore, electricity generation analyses showed the predominant role of the PV system, contributing 92.4% of total electricity generated, while wind turbines contributed 7.39%. The optimized electrolyzer yielded 111 877 kg of hydrogen annually with a mean capacity factor of 23.7%.

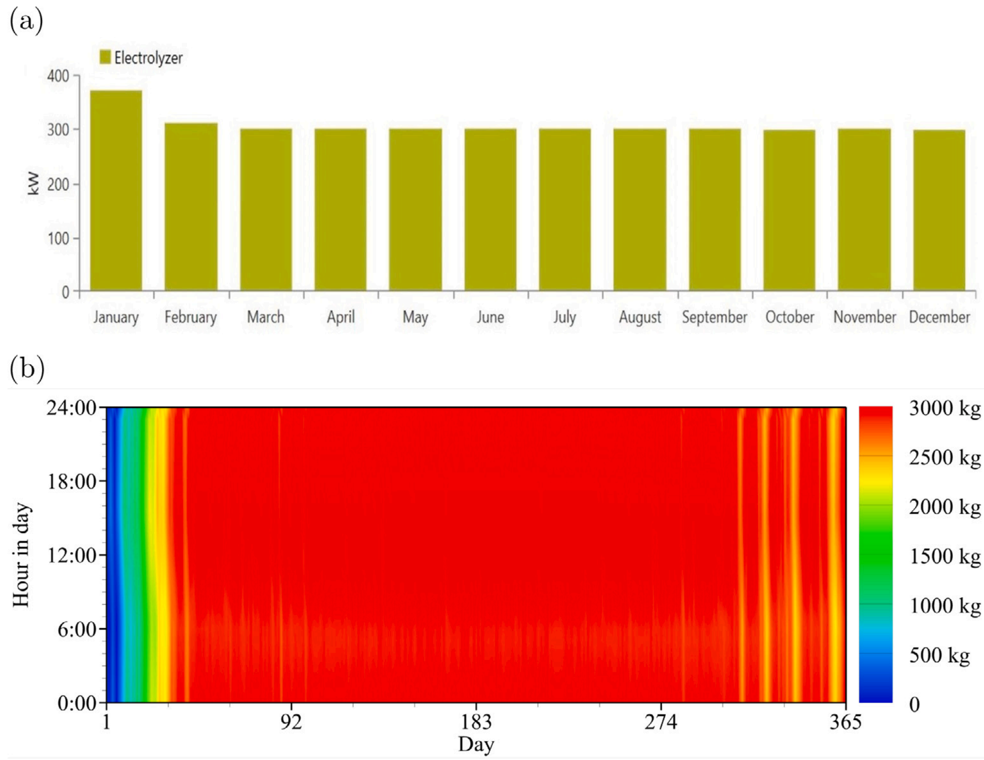

Fig. 11. (a) Monthly average electrolyzer input power. (b) Yearly (365/24) hydrogen tank level of the optimum system.

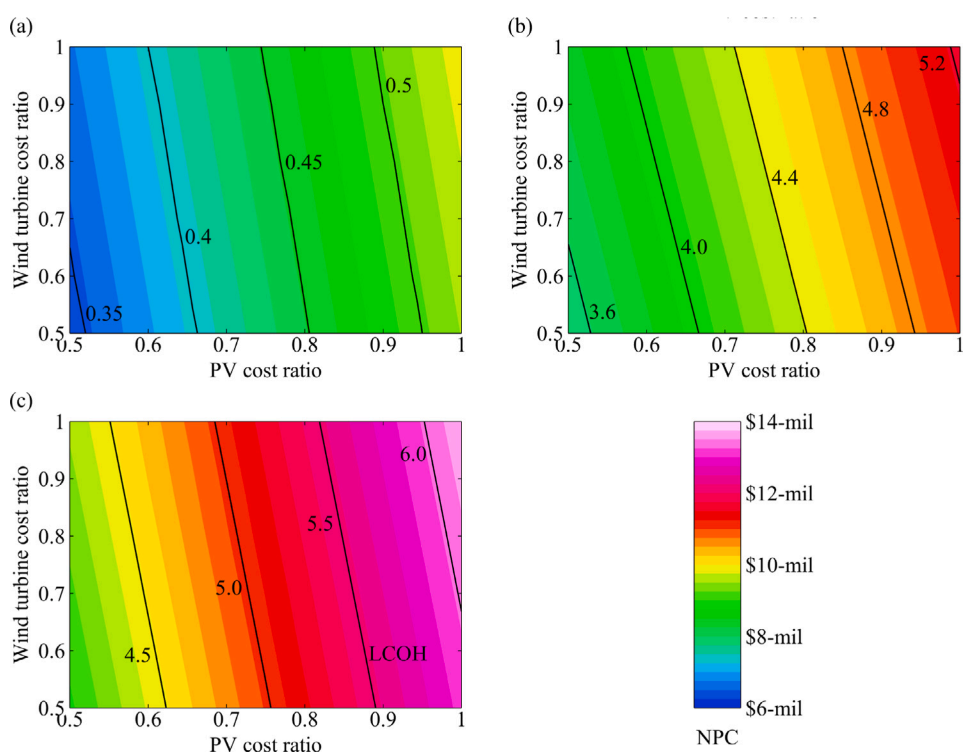

Fig. 12. Net present cost, NPC ($; flooded contours) overlaid with the levelized cost of hydrogen, LCOH ($/kg; contour lines) for systems (a) 1, (b) 2 and (c) 3.

The sensitivity analyses highlight the impacts of varying PV and wind turbine costs, electrolyzer lifetime, and electricity prices on the levelized costs of energy and hydrogen. It is found that Hydrogen production cost hinges on the levelized cost of energy, influenced by PV and wind turbine costs, with PV impacting LCOE more significantly than wind turbines. A 50% PV cost reduction led to a 32.3% LCOE decrease. Extending electrolyzer life reduces LCOH substantially by over 10%. Selling energy back to the grid affects hydrogen costs for grid-connected systems. A 50% increase in the tariff-in feed resulted in a nearly 6% drop in LCOH. In regions rich in renewable resources, a grid-connected PV-WT hybrid system demonstrated economic viability, providing insights into sustainable energy solutions.

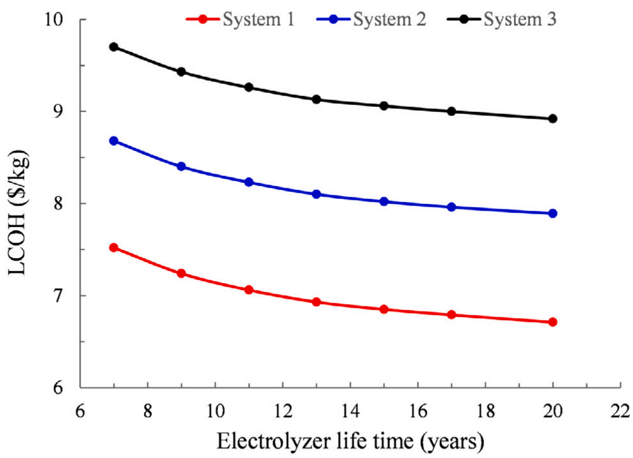

Fig. 13. Effect of the electrolyzer lifetime on LCOH.

Declaration of competing interest

The authors declare that they have no known competing financial interests or personal relationships that could have appeared to influence the work reported in this paper.

Acknowledgements

This work is funded in part by the Kuwait Foundation for the Advancement of Sciences (KFAS) under project code CN22-15SE-1612. The authors are grateful for the support of the Mechanical Engineering Department of the Australian University of Kuwait.

References

[1] Tarhan C, Çil MA. A study on hydrogen, the clean energy of the future: Hydrogen storage methods. J Energy Storage 2021;40:102676.
[2] Nasser M, Megahed TF, Ookawara S, Hassan H. Performance evaluation of PV panels/wind turbines hybrid system for green hydrogen generation and storage: Energy, exergy, economic, and enviroeconomic. Energy Convers Manage 2022;267:115870.
[3] Huang Q, Shi Y, Wang Y, Lu L, Cui Y. Multi-turbine wind-solar hybrid system. Renew Energy 2015;76:401–7.
[4] Ursúa A, Barrios EL, Pascual J, San Martín I, Sanchis P. Integration of commercial alkaline water electrolysers with renewable energies: Limitations and improvements. Int J Hydrogen Energy 2016;41:12852–61.
[5] Papadopoulos V, Desmet J, Knockaert J, Develder C. Improving the utilization factor of a PEM electrolyzer powered by a 15 MW PV park by combining wind power and battery storage–Feasibility study. Int J Hydrogen Energy 2018;43:16468–78.
[6] Qazi A, Hussain F, Rahim NA, Hardaker G, Alghazzawi D, Shaban K, et al. Towards sustainable energy: A systematic review of renewable energy sources, technologies, and public opinions. IEEE Access 2019;7:63837–51.
[7] Al-Enezi F, Sykulski J, Ahmed NA. Visibility and potential of solar energy on horizontal surface at Kuwait area. Energy Procedia 2011;862–72.
[8] Panwar NL, Kaushik SC, Kothari S. Role of renewable energy sources in environmental protection: A review. Renew Sustain Energy Rev 2011;15(3):1513–24.
[9] Yadav KK, Krishnan S, Gupta N, Prasad S, Amin MA, Cabral-Pinto MM, et al. Review on evaluation of renewable bioenergy potential for sustainable development: Bright future in energy practice in India. ACS Sustain Chem Eng 2021;9(48):16007–30.
[10] Steensma G, Román R, Marshall C, Bermejo J, Iyer K, Al-Hajraf S, et al. Shagaya renewable energy park project. In: AIP conference proceedings, vol. 2126, 2019, 040003.
[11] Majed A-R, Gueymard CA, Al-Khayat M, Ismail A, Lee JA, Al-Duaj H. Performance evaluation of a utility-scale dual-technology photovoltaic power plant at the Shagaya renewable energy park in Kuwait. Renew Sustain Energy Rev 2020;133:110139.
[12] Al-Dousari A, Al-Nassar W, Al-Hemoud A, Alsaleh A, Ramadan A, Al-Dousari N, et al. Solar and wind energy: Challenges and solutions in desert regions. Energy 2019;176:184–94.
[13] Naegele S, McCandless T, Greybush S, Young G, Haupt S, Al-Rasheedi M. Climatology of wind variability for the Shagaya region in Kuwait. Renew Sustain Energy Rev 2020;133:110089.
[14] International Energy Agency. Average annual capacity factors by technology. 2019.
[15] Akyuz E, Oktay Z, Dincer I. Performance investigation of hydrogen production from a hybrid wind-PV system. Int J Hydrogen Energy 2012;37:16623–30.
[16] Hasan MM, Genç G. Techno-economic analysis of solar/wind power based hydrogen production. Fuel 2022;324:124564.
[17] Alzahrani A, Ramu SK, Devarajan G, Vairavasundaram I, Vairavasundaram S. A review on hydrogen-based hybrid microgrid system: Topologies for hydrogen energy storage, integration, and energy management with solar and wind energy. Energies 2022;15:7979.
[18] Acakpovi A, Adjei P, Nwulu N, Asabere NY. Optimal hybrid renewable energy system: A comparative study of wind/hydrogen/fuel-cell and wind/battery storage. J Electr Comput Eng 2020;2020:1–15.
[19] Okonkwo PC, Barhoumi EM, Mansir IB, Emori W, Uzoma PC. Techno-economic analysis and optimization of solar and wind energy systems for hydrogen production: A case study. Energy Sourc, Part A: Recov, Util, Environ Effects 2022;44:9119–34.
[20] Al-Sharafi A, Sahin AZ, Ayar T, Yilbas BS. Techno-economic analysis and optimization of solar and wind energy systems for power generation and hydrogen production in Saudi Arabia. Renew Sustain Energy Rev 2017;69:33–49.
[21] Okonkwo PC, Mansir IB, Emori W, Radwan AB, Shakoor RA, Uzoma PC, et al. Utilization of renewable hybrid energy for refueling station in Al-Kharj, Saudi Arabia. Int J Hydrogen Energy 2022;47:22273–84.
[22] Nasser M, Megahed TF, Ookawara S, Hassan H. A review of water electrolysis–based systems for hydrogen production using hybrid/solar/wind energy systems. Environ Sci Pollut Res 2022;1–25.
[23] Al-Nassar W, Alhajraf S, Al-Enizi A, Al-Awadhi L. Potential wind power generation in the State of Kuwait. Renew Energy 2005;30:2149–61.
[24] Hadi MA, Abdel-Razek R, Chakroun WM. Economic assessment of the use of solar energy in Kuwait. Glob J Bus Res 2013;7:73–82.
[25] Muhaisen NA, Ahmed MM, Khan S, Habaebi MH, Ahmed NA, Arshad A. Development of renewable energy potential in Kuwait. In: 2016 IEEE student conference on research and development. SCOReD, 2016, p. 1–4.
[26] Al-Nassar WK, Neelamani S, William TS. Economic feasibility of wind and photovoltaic energy in Kuwait. In: E3S web of conferences, vol. 280, 2021, p. 05016.
[27] Alawadhi EM. The potential of wind energy in Kuwait: A complete feasibility investigation. J Eng Res 2023;11.
[28] Bedoud K, Ali-Rachedi M, Lakel R. Assessment and analysis of wind energy generation and power control of wind turbine system. Synthèse: Rev des Sci et de la Technol 2016;32:147–62.
[29] Guo S, Liu Q, Sun J, Jin H. A review on the utilization of hybrid renewable energy. Renew Sustain Energy Rev 2018;91:1121–47.
[30] Hussam WK, Khlefat AM, Sheard GJ. Energy saving and performance analysis of air-cooled photovoltaic panels. Int J Energy Res 2022;46:4825–34.
[31] Pricing, output, and returns. Solar choice solar PV energy system installation brokers. 5 kW solar systems pricing output and returns comments. 2021, Solar Choice.
[32] Mazloomi S, Sulaiman N. Influencing factors of water electrolysis electrical efficiency. Renew Sustain Energy Rev 2012;16:4257–63.
[33] García P, Torreglosa JP, Fernández LM, Jurado F. Improving long-term operation of power sources in off-grid hybrid systems based on renewable energy, hydrogen and battery. J Power Sources 2014;265:149–59.
[34] Rahman S, Tam K-s. A feasibility study of photovoltaic-fuel cell hybrid energy system. IEEE Trans Energy Convers 1988;3:50–5.
[35] National Renewable Energy Laboratory. HOMER Pro® microgrid software. 2019.
[36] Ma T, Yang H, Lu L. A feasibility study of a stand-alone hybrid solar–wind–battery system for a remote island. Appl Energy 2014;121:149–58.
[37] Abdin Z, Mérida W. Hybrid energy systems for off-grid power supply and hydrogen production based on renewable energy: A techno-economic analysis. Energy Convers Manag 2019;196:1068–79.
[38] Rezk H, Alghassab M, Ziedan HA. An optimal sizing of stand-alone hybrid PV-fuel cell-battery to desalinate seawater at saudi NEOM City. Processes 2020;8(4):382.
[39] Kapen PT, Nouadje BAM, Chegnimonhan V, Tchuen G, Tchinda R. Techno-economic feasibility of a PV/battery/fuel cell/electrolyzer/biogas hybrid system for energy and hydrogen production in the far north region of cameroon by using HOMER pro. Energy Strategy Rev 2022;44:100988.
[40] Hussam WK, Salem HJ, Redha AM, Khlefat AM, Al Khatib F. Experimental and numerical investigation on a hybrid solar chimney-photovoltaic system for power generation in Kuwait. Energy Convers Manag.: X 2022;15:100249.
[41] Chen Q, Gu Y, Tang Z, Wang D, Wu Q. Optimal design and techno-economic assessment of low-carbon hydrogen supply pathways for a refueling station located in shanghai. Energy 2021;237:121584.
[42] Samy M, Barakat S, Ramadan H. A flower pollination optimization algorithm for an off-grid PV-fuel cell hybrid renewable system. Int J Hydrogen Energy 2019;44(4):2141–52.

[43] Güven AF, Yörükeren N, Samy MM. Design optimization of a stand-alone green energy system of university campus based on Jaya-Harmony search and ant colony optimization algorithms approaches. Energy 2022;253:124089.

[44] Thirunavukkarasu M, Sawle Y, Lala H. A comprehensive review on optimization of hybrid renewable energy systems using various optimization techniques. Renew Sustain Energy Rev 2023;176:113192.